^{207}Pb-^{206}Pb dating of magnetite, monazite and allanite in the central and northern Nagssugtoqidian orogen, West Greenland

Henrik Stendal, Karsten Secher and Robert Frei

Pb-isotopic data for magnetite from amphibolites in the Nagssugtoqidian orogen, central West Greenland, have been used to trace their source characteristics and the timing of metamorphism. Analyses of the magnetite define a Pb-Pb isochron age of 1726 ± 7 Ma. The magnetite is metamorphic in origin, and the 1726 Ma age is interpreted as a cooling age through the closing temperature of magnetite at ~600°C. Some of the amphibolites in this study come from the Naternaq supracrustal rocks in the northern Nagssugtoqidian orogen, which host the Naternaq sulphide deposit and may be part of the Nordre Strømfjord supracrustal suite, which was deposited at around 1950 Ma ago.

Pb-isotopic signatures of magnetite from the Arfersiorfik quartz diorite in the central Nagssugtoqidian orogen are compatible with published whole-rock Pb-isotopic data from this suite; previous work has shown that it is a product of subduction-related calc-alkaline magmatism between 1920 and 1870 Ma. Intrusion of pegmatites occurred at around 1800 Ma in both the central and the northern parts of the orogen. Pegmatite ages have been determined by Pb stepwise leaching analyses of allanite and monazite, and source characteristics of Pb point to an origin of the pegmatites by melting of the surrounding late Archaean and Palaeoproterozoic country rocks. Hydrothermal activity took place after pegmatite emplacement and continued below the closure temperature of magnetite at 1800–1650 Ma. Because of the relatively inert and refractory nature of magnetite, Pb-isotopic measurements from this mineral may be of help to understand the metamorphic evolution of geologically complex terrains.

Keywords: Pb isotopes, magnetite, Nagssugtoqidian orogen, Palaeoproterozoic, pegmatites, Pb stepwise leaching, supracrustal rocks

---

H.S. & K.S., *Geological Survey of Denmark and Greenland, Øster Voldgade 10, DK-1350 Copenhagen K, Denmark.*
E-mail: *hst@geus.dk*
R.F., *Geological Institute, University of Copenhagen, Øster Voldgade 10, DK-1350 Copenhagen K, Denmark.*

As part of the research programme 2000–2003 in the Nagssugtoqidian orogen of West Greenland by the Geological Survey of Denmark and Greenland (GEUS), an assessment was made of the mineral resource potential of the region between Maniitsoq (Sukkertoppen; 66°N) and the southern part of Nuussuaq (70°15′N; Stendal *et al.* 2004). The present study comprises Pb-isotopic analyses of magnetite from amphibolites, hydrothermally altered amphibolites, the Arfersiorfik quartz diorite (see below), skarn, ultramafic rocks and pegmatites. Magnetite was chosen as a medium for analysis because of its abundance in amphibolites, even though the concentration of Pb in magnetite is generally low. In addition, an attempt was made to date monazite and allanite from pegmatites by the Pb stepwise leaching (PbSL) technique (Frei & Kamber 1995). The Pb-isotopic study of the amphibolites covers the Attu, Kangaatsiaq and Qasigiannguit regions (Fig. 1). The analysed pegmatites are from the Nordre

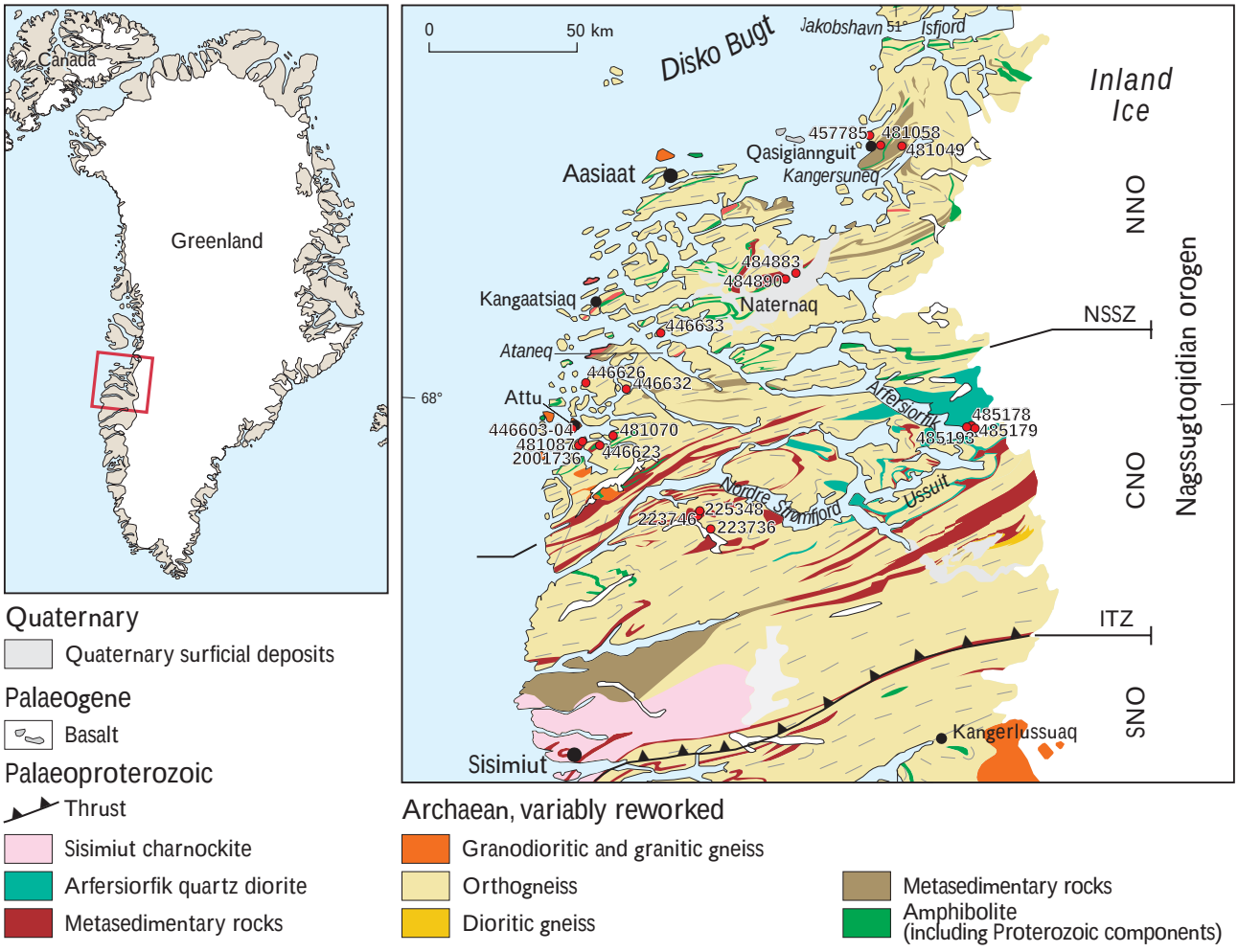

Fig. 1. Geological map of central West Greenland, modified from van Gool *et al.* (2002). Red dots with numbers refer to samples analysed. CNO, Central Nagssugtoqidian orogen; NNO, Northern Nagssugtoqidian orogen; SNO, Southern Nagssugtoqidian orogen; ITZ, Ikertôq thrust zone; NSSZ, Nordre Strømfjord shear zone.

Strømfjord (Nassuttooq), Attu and Qasigiannguit areas. The aims of the study were (1) to use Pb-isotopic signatures of magnetite in an attempt to outline the metamorphic history of the region; (2) to characterise the hydrothermal overprinting in terms of its timing and Pb source; and (3) to place the results within the evolutionary frame of the Nagssuqtoqidian orogen.

Regional geological setting

The study region comprises the Palaeoproterozoic Nagssugtoqidian orogen, a major collisional belt situated just north of the North Atlantic Craton (van Gool *et al.* 2002), as well as the southernmost part of the contemporaneous Rinkian fold belt (Garde & Steenfelt 1999; Connelly *et al.* 2006). Most of the region consists of Archaean orthogneisses, variably reworked during the Nagssugtoqidian and Rinkian tectonothermal events. Several thin belts of supracrustal rocks occur within the reworked Archaean gneiss terrain of the Nagssugtoqidian orogen (Fig. 1). Granitoid rocks and numerous pegmatites intrude the gneisses. Formations of Palaeoproterozoic age are limited to the Sisimiut igneous suite, Arfersiorfik quartz diorite, and minor supracrustal sequences including the Naternaq supracrustal belt (Connelly *et al.* 2000; Thrane & Connelly 2006, this volume).

The metamorphic grade is amphibolite facies, except for an area south of Ataneq in the south-western part of the northern Nagssugtoqidian orogen (NNO; Fig. 1) and in most of the central Nagssugtoqidian orogen (CNO), where granulite facies rocks predominate. The gneisses are intensely folded and show a general E–W to NE–SW strike. Deformation of the Archaean gneisses in the NNO

decreases gradually northwards, from high-strain to more open structures in the Archaean rocks. Steeply and shallowly dipping shear and fault zones are common in contact zones between different rock types. Major fault and shear zones generally strike NNE–NE. The gneisses of the NNO are late Archaean, with ages between 2870 and 2700 Ma (Kalsbeek & Nutman 1996; Connelly & Mengel 2000; Thrane & Connelly 2006, this volume). However, older rocks with ages ~3150 Ma appear to be present in the Attu area (Stendal *et al*. 2006, this volume). Only a few younger Palaeoproterozoic ages have been obtained from the NNO, including an undeformed pegmatite between Attu and Aasiaat with an intrusion age of about 1790 Ma (Connelly & Mengel 2000).

The geological history of the study area can be summarised as follows (van Gool *et al*. 2002):

- Deposition of supracrustal rocks: 2200–1950 Ma
- Continental breakup – the Kangâmiut dyke swarm: 2040 Ma
- Drifting – sediment deposition (supracrustal rocks) in the Nordre Strømfjord area: 2000–1920 Ma
- Subduction – calc-alkaline magmatism, giving rise to the Sisimiut and Arfersiorfik igneous suites: 1920–1870 Ma
- Peak metamorphism during collision (D1 and D2): 1860–1840 Ma
- Large scale folding (D3): ~1825 Ma
- Shearing in steep belts (D4): ~1775 Ma
- Slow cooling following the shearing, with closing temperature of rutile (420°C) at around 1670 Ma (Connelly *et al.* 2000). Based on ^{40}Ar-^{39}Ar and U-Pb data for several minerals, Willigers *et al.* (2001) estimated cooling temperatures around 500°C at ~1700 Ma, 410°C at ~1640 Ma, and 200°C at ~1400 Ma.

Previous investigations

The Geological Survey, university research groups as well as exploration companies have been working in central West Greenland for decades and have collected significant amounts of data on the mineral potential of the region (Stendal *et al*. 2002, 2004; Stendal & Schønwandt 2003; Schjøth & Steenfelt 2004; Steenfelt *et al*. 2004). Whole-rock Pb-Pb, Rb-Sr and Sm-Nd isotopic data from the study area have been presented by Kalsbeek *et al.* (1984, 1987, 1988), Taylor & Kalsbeek (1990) and Whitehouse *et al.* (1998), while e.g. Kalsbeek & Nutman (1996), Connelly & Mengel (2000), Connelly *et al.* (2000), Hollis *et al*. (2006, this volume) and Thrane & Connelly (2006, this volume) have published zircon U-Pb geochronological data.

Pb-isotopic work has been carried out on sulphide separates, mainly pyrite, from a mineralisation in the Disko Bugt region north of the study area (Stendal 1998). In the latter study, two distinct mineralisation types in the Archaean rocks were identified – a syngenetic, and at least one epigenetic type of ore formation. Pb-isotopic data of sulphides from Proterozoic rocks yield a well-defined linear trend in a Pb-Pb isochron diagram, with a slope corresponding to an age of ~1900 Ma, and indicative of a primitive (i.e. low μ) source character of Pb in that mineralisation.

Local geology and descriptions of the investigated rocks

During this study Pb-isotopic analyses were carried out on magnetite from amphibolite (four samples), banded iron formation (one sample), hydrothermally altered amphibolite and calc-silicate skarn rock (four samples), the Arfersiorfik quartz diorite (three samples), magnetite skarn (one sample), ultramafic rock (one sample) and pegmatite (one sample). In addition, one amphibolite, one altered amphibolite and one sample of banded iron formation were subjected to PbSL procedures (Frei & Kamber 1995), and allanite (two samples) and monazite (three samples) from pegmatites were analysed by PbSL in an attempt to date their emplacement. Brief descriptions of the investigated rocks are given below.

Amphibolitic rocks

Amphibolites occur together with garnet-mica schists/gneisses in supracrustal sequences, interlayered with orthogneiss. Some amphibolite layers in the gneiss terrain can be followed continuously along strike for up to tens of kilometres. They are heterogeneous in composition. They are found in three associations: (1) rusty weathering, medium-grained garnet amphibolite layers (*c*. 0.5 m thick) folded together with the orthogneisses, (2) dark, fine-grained amphibolite, occurring as layers up to 10 m thick, and (3) medium-grained, commonly garnetiferous, layered amphibolite. Layered amphibolites are the most common, and occur as units up to 200 m thick, although layers only 10–20 m thick are more common. The three different types of amphibolite form separate outcrops and do not occur together. The Pb-isotopic analyses reported in this paper refer to magnetite from the layered amphibolites (type 3).

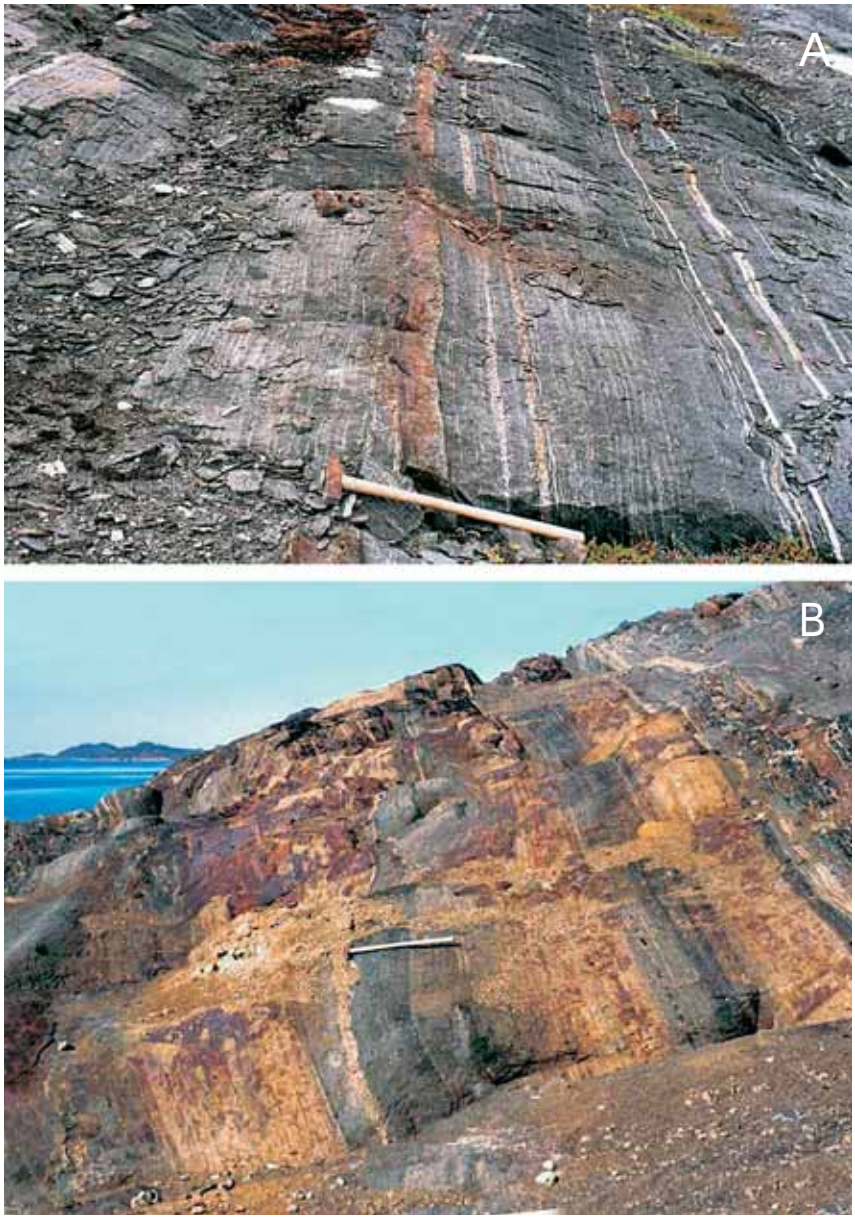

Fig. 2. Amphibolite (A) and hydrothermally altered amphibolite (B) from the Attu area.

The supracrustal sequences consist of garnet-mica schist/gneiss, together with amphibolite (Fig. 2a) and rusty weathering layers *c*. 1 m thick of quartz-garnet rich gneiss with some iron sulphides (1 vol.%). Within the layered amphibolite sequences, magnetite-bearing horizons 1–10 m thick occur. The magnetite occurs in laminae 1–10 mm thick, alternating with quartz-feldspar laminae of the same thickness. Alteration is common within the layered amphibolites.

Altered amphibolite

Some amphibolites have been hydrothermally altered and sulphide mineralised and may contain calc-silicates. This type of amphibolite is dominated by layered garnet-rich amphibolite, interlayered with magnetite-bearing and rusty weathering layers, with disseminated pyrite (Fig. 2b). The layers are generally 0.5–2 m thick; in some cases layered amphibolite is intercalated with rusty weathering layers 10–30 cm thick, consisting of quartz-bearing mica schist with iron sulphides and staining of malachite. Within the altered amphibolite calc-silicate minerals are found in zones 1–2 m thick or as smaller lenses, comprising hornblende, diopside, garnet and magnetite.

Fig. 3. Banded iron formation sequence from the Naternaq area.

Banded iron formation at Naternaq

The supracrustal belt at Naternaq (Fig. 1) consists of metavolcanic rocks interlayered with pelitic and psammitic schists and gneisses, marble units, exhalites and chert-rich layers with minor quartzite and banded iron formation. In total, these units define a supracrustal sequence up to 3 km thick, which is folded into a major shallowly dipping WSW-trending antiform. The supracrustal sequence can be traced for approximately 30 km along strike and is intruded by granite sheets and pegmatite veins. Østergaard *et al.* (2002) and Stendal *et al.* (2002) give detailed descriptions of the stratigraphy of the supracrustal rocks. The banded iron formation (Fig. 3) occurs locally associated with the amphibolite in zones composed of centimetre-thick layers of magnetite and siderite quartz and calc-silicates. The depositional environment is of a sedimentary type comprising true sediments, submarine volcanic rocks and exhalites. A range of variably altered conformable horizons of very fine-grained siliceous and sulphide rich lithologies associated with either amphibolite or marble are interpreted as volcanogenic-exhalitic rocks (Østergaard *et al*. 2002; Stendal *et al.* 2002).

Arfersiorfik quartz diorite

The Arfersiorfik quartz diorite (Kalsbeek *et al.* 1987) is located in the eastern part of the fjord Arfersiorfik (Fig. 1) and covers several hundreds of square kilometres. Within the quartz diorite body, magnetite occurs in hornblende-rich rocks (hornblende, quartz, feldspar, and chlorite) and often shows paragenetic relation with iron sulphides (predominantly pyrrhotite). The Arfersiorfik quartz diorite was emplaced in the period 1920–1870 Ma (Kalsbeek *et al.* 1987; Connelly *et. al.* 2000).

Ultramafic rocks near Qasigiannguit

An ultramafic body 300 × 300 m large is located on the north side of Kangersuneq, forming rusty weathered hills. On its eastern and western sides the ultramafic body is bounded by fault zones, invaded by pegmatites. On its northern and southern sides it is bordered by amphibolite and garnet amphibolite, respectively. Because of the penetrative weathering it is difficult to sample fresh material from the ultramafic body. In its centre, an intensely rusty weathered and eroded 'joint' zone cuts the ultramafic rocks. This contains 1–10 vol.% magnetite.

Magnetite-rich skarn at Qasigiannguit

Near Qasigiannguit a skarn rock is found in the contact zone striking 66° and dipping 77°SE between mica schist and quartzite and a marble-calc-silicate sequence. It comprises magnetite skarn (0.5 m thick) in close contact with the mica schist and quartzite. Towards the south-east the magnetite skarn is followed by alternating layers of calc-silicate rocks and marble (including a quartzitic, sulphide-rich layer), followed by a pegmatite body.

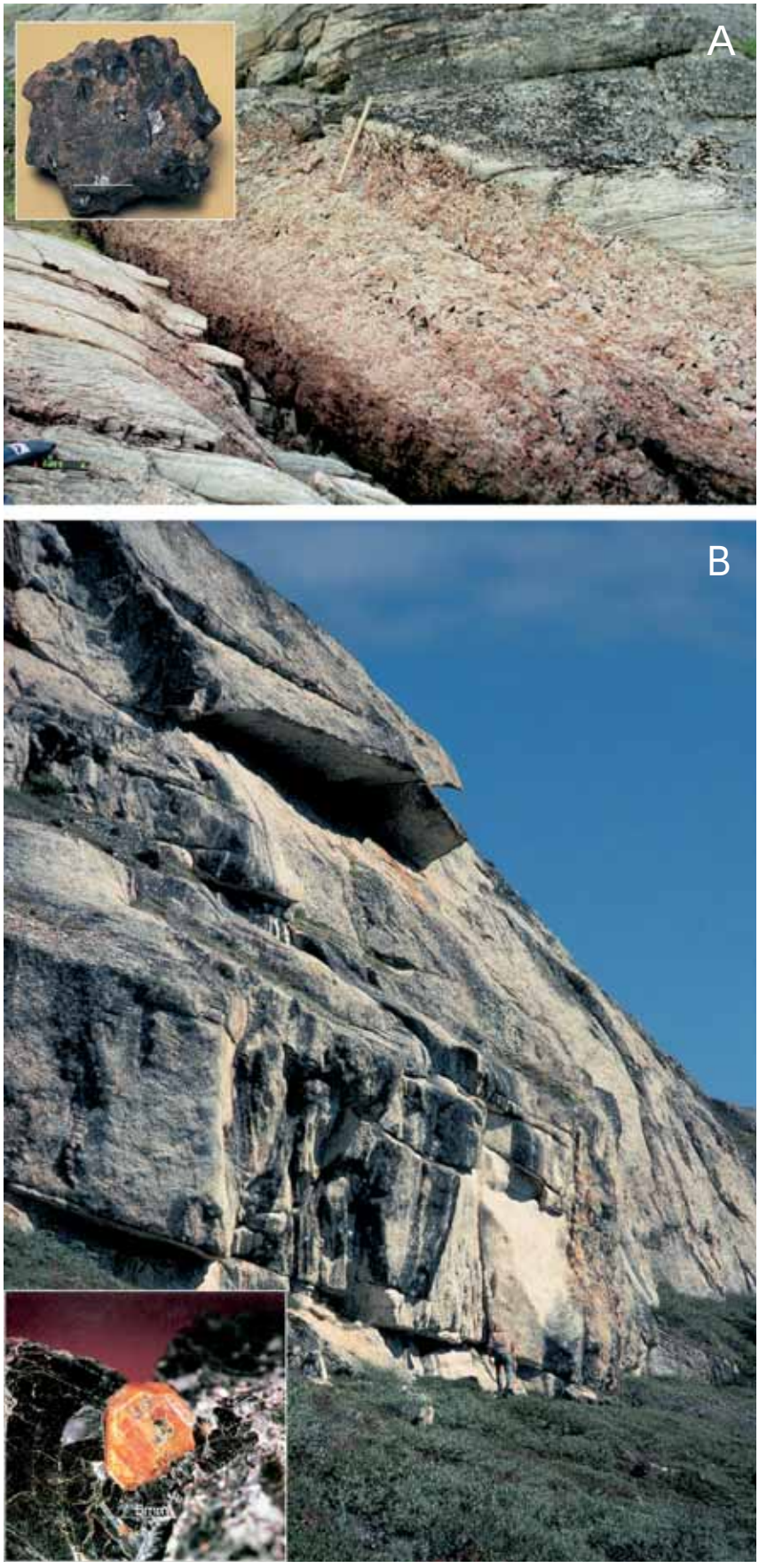

Fig. 4. Pegmatites and minerals analysed. A: Pink discordant pegmatite and allanite (inset) from the Attu area. B: White pegmatite and monazite (inset) from the Nordre Strømfjord (Nassuttooq) area.

Pegmatites

Pink pegmatites. Throughout the study area, especially in the outer fjord zone from south of Attu northward to Kangaatsiaq, the country rocks are intruded by granite and by pink pegmatites with alkali feldspar crystals commonly more than 10 cm in size. The pegmatites occur mostly as discordant decimetre- to metre-thick bodies within the gneisses, at contacts between major lithological units, and within supracrustal rocks where they are clearly cross-cutting. The dominant minerals in the pink pegmatite are alkali feldspar, quartz, biotite and subordinate allanite, titanite, apatite, magnetite and Fe-sulphides (Fig. 4a). Zonation is occasionally seen with quartz-rich centres bounded by alkali feldspar-rich parts.

White pegmatites. White pegmatites are generally concordant (but locally discordant) to the foliation of the adjacent country rocks, typically grey gneiss and supracrustal rocks. The pegmatites are 5–20 m wide and 50–200 m long with a general trend of NW–SE all over the Nordre Strømfjord and Ussuit areas. Gradational contacts to the host rocks are common. Quartz and feldspar dominate the white pegmatites, with garnet, biotite, monazite, magnetite and zircon as characteristic minor constituents. Monazite is found as 0.5–5 mm orange crystals that mainly occur in plagioclase- and biotite-rich pegmatites (Fig. 4b). Monazite crystals are euhedral and occur in lens-shaped layers accompanied by biotite, set in a granoblastic matrix of primarily plagioclase (Secher 1980).

Analytical methods

Pb isotope analyses for this study were carried out at the Danish Centre for Isotope Geology, Geological Institute, University of Copenhagen. Mineral fractions were separated from dry split aliquots of crushed and sieved (100–200 µm) rock powders using a hand magnet, a Frantz isodynamic separator and heavy liquid techniques. No further purification was carried out, and the mineral fractions may contain minor proportions of foreign minerals. Pb was separated conventionally on 0.5 ml glass columns charged with anion exchange resin, followed by a clean up on 200 µl Teflon columns. A standard HBr-HCl solution recipe was applied in both column steps. Total procedural blanks for Pb amounted to < 120 pg which is considered insignificant for the measured Pb-isotopic results, relative to the amount of sample Pb estimated from the mass spectrometer signal intensities. Isotope analyses were

Table 1. Pb isotope ratios of magnetite from different rock types

Sample	Locality	Latitude N	Longitude W	Rock	$^{206}Pb/^{204}Pb$	± 2σ*	$^{207}Pb/^{204}Pb$	± 2σ	$^{208}Pb/^{204}Pb$	± 2σ	r1 **	r2†
Magnetite from amphibolite and banded iron formation												
446626	Ataneq	68°.061	53°.510	Amphibolite	18.815	0.026	15.549	0.022	44.971	0.068	0.973	0.953
446632	Ataneq	68°.047	53°.179	Amphibolite	28.204	0.042	16.518	0.026	38.467	0.066	0.971	0.906
446623	Attu	67°.837	53°.408	Amphibolite	17.522	0.025	15.404	0.024	38.344	0.066	0.961	0.880
481070	Attu	67°.915	53°.231	Amphibolite	17.388	0.019	15.376	0.018	41.241	0.053	0.978	0.936
484883	Naternaq	68°.398	51°.941	BIF in amphibolite	54.587	0.028	19.316	0.012	36.871	0.030	0.942	0.886
Magnetite from altered amphibolite and calc-silicate rock												
446633	Niaqornaarsuk	68°.217	53°.028	Altered amphibolite	26.387	0.505	16.465	0.316	47.423	0.908	0.998	0.999
446603	Attu	67°.927	53°.622	Altered amphibolite	18.398	0.030	15.620	0.026	41.710	0.074	0.978	0.956
446604	Attu	67°.927	53°.622	Altered amphibolite	18.256	0.046	15.638	0.042	40.443	0.122	0.930	0.845
484890	Naternaq	68°.408	51°.935	Calc-silicates (skarn)	16.534	0.009	15.372	0.010	35.562	0.028	0.957	0.913
Magnetite from the Arfersiorfik quartz diorite												
485178	Arfersiorfik	67°.970	50°.430	Quartz diorite	17.790	0.016	15.469	0.016	36.703	0.049	0.919	0.782
485179	Arfersiorfik	67°.967	50°.412	Quartz diorite	18.071	0.018	15.498	0.016	36.343	0.041	0.975	0.954
485193	Arfersiorfik	67°.956	50°.594	Hornblenditic rock	17.007	0.013	15.456	0.013	37.124	0.037	0.959	0.902
Magnetite from pegmatite												
481087	Attu	67°.890	53°.517	Pegmatite	28.393	0.043	16.602	0.026	189.024	0.311	0.982	0.971
Magnetite from ultramafic rock and skarn												
481049	Qasigiannguit	68°.801	50°.973	Ultramafic rock	25.827	0.039	16.103	0.025	51.334	0.084	0.979	0.949
481058	Qasigiannguit	68°.800	51°.169	Magnetite skarn	35.124	0.024	17.028	0.013	38.847	0.035	0.968	0.929

BIF: Banded iron formation.

* Errors are 2σ absolute (Ludwig 1990).

** r1 = $^{206}Pb/^{204}Pb$ versus $^{207}Pb/^{204}Pb$ error correlation (Ludwig 1990).

† r2 = $^{206}Pb/^{204}Pb$ versus $^{208}Pb/^{204}Pb$ error correlation (Ludwig 1990).

Table 2. Pb-Pb step leaching data for magnetite, allanite, and monazite in banded iron formation, amphibolite and pegmatites in the Nagssugtoqidian orogen

Code	Acid	Time	$^{206}Pb/^{204}Pb$	± 2σ *	$^{207}Pb/^{204}Pb$	± 2σ *	$^{208}Pb/^{204}Pb$	± 2σ *	r1	r2
Magnetite, banded iron formation within amphibolite 484883, locality 68°.398 N, 51°.941 W										
[1]	1 N HBr	30'	48.234	0.030	18.615	0.014	37.418	0.032	0.968	0.919
[2]	1 N HBr	1 h	120.002	0.091	26.407	0.022	3.862	0.005	0.978	0.760
[3]	4 N HBr	3 h	94.120	0.363	23.247	0.090	37.841	0.149	0.995	0.987
[4]	8 N HBr	6 h	30.176	0.239	16.809	0.134	35.387	0.282	0.994	0.994
[5]	8 N HBr	12 h	18.799	0.062	15.506	0.052	34.534	0.116	0.991	0.987
[6]	HF	12 h	18.799	0.124	15.539	0.103	35.013	0.233	0.995	0.993
Magnetite, amphibolite 446632, locality 68°.047 N, 53°.179 W										
[1]	1 N HBr	30'	19.932	0.026	15.621	0.021	37.462	0.055	0.970	0.920
[2]	1 N HBr	1 h	38.765	0.032	17.639	0.016	39.167	0.040	0.978	0.946
[3]	4 N HBr	3 h	35.439	0.060	17.098	0.030	42.830	0.079	0.982	0.948
[4]	8 N HBr	6 h	37.099	0.150	17.595	0.072	36.972	0.154	0.993	0.979
[5]	8 N HBr	12 h	40.431	0.219	18.100	0.099	34.544	0.189	0.994	0.994
[6]	HF	12 h	28.265	0.083	16.910	0.051	34.598	0.106	0.987	0.977
Magnetite, altered amphibolite 446633, locality 68°.217 N, 53°.027 W										
[1]	1 N HBr	30'	25.206	0.021	16.298	0.015	45.932	0.047	0.971	0.914
[2]	1 N HBr	1 h	27.276	0.170	16.492	0.104	47.555	0.300	0.993	0.990
[3]	4 N HBr	3 h	25.359	0.022	16.261	0.016	45.944	0.049	0.975	0.948
[4]	8 N HBr	6 h	26.018	0.024	16.333	0.016	46.646	0.051	0.968	0.936
[5]	8 N HBr	12 h	27.705	0.073	16.539	0.046	48.236	0.138	0.965	0.937
Allanite, pegmatite 2001-736, locality 67°.883 N, 53°.523 W										
[1]	1 N HBr	30'	22.579	0.029	15.860	0.021	137.787	0.193	0.982	0.960
[2]	1 N HBr	1 h	21.528	0.013	15.728	0.011	123.978	0.101	0.971	0.939
[3]	4 N HBr	3 h	79.398	1.929	22.265	0.542	1360.842	33.070	0.999	1.000
[4]	8 N HBr	6 h	2527.779	37.253	295.424	4.391	52501.990	774.512	0.992	0.999
[5]	8 N HBr	12 h	7804.112	133.916	882.216	15.164	161163.864	2767.112	0.999	1.000
[6]	HF	12 h	551.839	2.322	74.260	0.322	11002.171	46.823	0.973	0.994
[7]	HF	2 d	111.336	0.543	25.175	0.136	1948.881	9.628	0.901	0.991
Allanite, pegmatite 457785, locality 68°.834 N, 51°.226 W										
[1]	1 N HBr	30'	36.910	1.617	17.616	0.772	538.548	23.595	1.000	1.000
[2]	1 N HBr	1 h	44.614	0.389	18.318	0.160	714.245	6.237	0.998	0.999
[3]	4 N HBr	3 h	26.321	0.210	16.341	0.130	270.923	2.164	0.998	0.999
[4]	8 N HBr	6 h	21966.303	527.491	2410.934	57.939	328786.908	7897.797	0.999	1.000
[5]	8 N HBr	12 h	26.193	0.574	17.165	0.390	161.467	3.639	0.964	0.972
[6]	HF	12 h	15.058	1.448	15.006	1.443	39.562	3.805	1.000	1.000
[7]	HF	2 d	27.000	0.230	15.806	0.207	186.650	2.183	0.651	0.729
Monazite, pegmatite 223736, locality 67°.680 N, 52°.565 W										
[1]	1 N HBr	30'	136.776	2.665	28.301	0.574	6619.883	131.103	0.960	0.984
[2]	1 N HBr	1 h	222.475	3.796	37.330	0.643	12548.515	214.343	0.991	0.999
[3]	4 N HBr	3h	219.227	2.039	36.918	0.346	12871.792	120.474	0.992	0.995
[4]	8 N HBr	6 h	184.897	2.055	33.259	0.373	10581.910	118.035	0.993	0.997
[5]	8 N HBr	12 h	89.680	0.811	23.046	0.213	3554.756	32.275	0.979	0.998
[6]	HF	12 h	39.412	0.038	17.328	0.018	88.489	0.099	0.980	0.957
[7]	HF	2 d	261.196	1.366	41.737	0.220	175.006	0.931	0.994	0.987
Monazite, pegmatite 223746, locality 67°.674 N, 52°.456 W										
[1]	1 N HBr	30'	20.955	0.097	15.264	0.071	156.248	0.733	0.995	0.994
[2]	1 N HBr	1 h	26.768	0.169	16.158	0.103	315.778	2.010	0.997	0.997
[3]	4 N HBr	3h	215.079	2.560	37.781	0.451	5263.963	62.733	0.997	0.999
[4]	8 N HBr	6 h	2978.834	188.060	343.540	21.694	75533.892	4768.946	1.000	1.000
[5]	8 N HBr	12 h	6392.913	99.502	721.057	11.259	157988.821	2460.811	0.997	1.000
[6]	HF	12 h	468.603	5.974	66.525	0.919	10731.171	137.428	0.923	0.996
[7]	HF	2 d	2161.547	97.250	254.541	11.458	51062.309	2297.561	1.000	1.000
Monazite, pegmatite 225348, locality 67°.833 N, 52°.323 W										
[1]	1 N HBr	30'	139.662	2.160	29.676	0.459	1656.012	25.630	1.000	1.000
[2]	1 N HBr	1 h	140.039	1.416	29.481	0.299	1544.411	15.642	0.996	0.999
[3]	4 N HBr	3h	877.104	4.121	108.678	0.517	12440.807	58.889	0.990	0.997
[4]	8 N HBr	6 h	25.459	0.418	16.750	0.456	225.146	4.515	0.604	0.820
[5]	8 N HBr	12 h	40549.054	1970.494	4458.008	222.550	602889.998	29313.071	0.973	1.000
[6]	HF	12 h	8037.949	261.731	893.317	29.098	122611.734	3993.108	1.000	1.000
[7]	HF	2 d	4389.260	60.969	493.058	6.880	66031.253	918.275	0.996	0.999

* Errors are 2σ absolute (Ludwig 1990). For explanations of r1 and r2, see Table 1.

Table 3. Pb isotope ages, μ1-values, and intercepts with the Stacey & Kramers (1975) Pb-isotopic growth curve for magnetite, allanite, and monazite from amphibolite, BIF and pegmatites

Sample	Rock	Mineral	Method	Age (Ma)	± 2σ	MSWD	Intercept (Ma) with Stacey & Kramers (1975)	μ1	± 2σ
5 samples	Amphibolite/BIF	Magnetite	Bulk	1726	6.5	1.38	2140	7.89	0.02
484883	BIF	Magnetite	PbSL	1756	36	8.70	2401	7.7	0.11
223736	Pegmatite	Monazite	PbSL	1797	13	4.44	2925	7	0.05
223746	Pegmatite	Monazite	PbSL	1816	16	41.7	2784	7.24	0.12
225348	Pegmatite	Monazite	PbSL	1787	11	76.9	2271	7.81	1.00
447783	Pegmatite	Allanite	PbSL	1785	9.2	12.9	2335	7.76	0.00
2001-736	Pegmatite	Allanite	PbSL	1818	12	53.8	2453	7.66	0.02

BIF: Banded iron formation; PbSL: Pb step leaching.

carried out on a VG Sector 54-IT instrument. Fractionation for Pb was controlled by repetitive analysis of the NBS 981 standard (values of Todt *et al*. 1993) and amounted to 0.103 ± 0.007% / amu (2 σ; n = 11). Stepwise Pb leaching (PbSL) experiments followed methods described in Frei & Kamber (1995).

The programmes and parameters of Ludwig (1990) were used for the isochron calculations. Model first-stage μ_1 values were calculated using 4.55 Ga for the age of the earth. All age and isotope data in this paper are given with 2 σ precisions.

Results

The Pb-isotopic results are given in Tables 1–3. The uranogenic Pb-isotopic composition of magnetite from the amphibolites (four samples; squares in Fig. 5) together with the banded iron formation (Naternaq; one sample outside the range of Fig. 5) define an isochron with an age of 1726 ± 7 Ma (2 σ; MSWD = 1.4; model μ_1 = 7.89 ± 0.02), which corresponds to a late stage in the metamorphic evolution of the Nagssugtoqidian orogen (cf. Willigers *et al*. 2002). This isochron intercepts the Stacey & Kramers (1975) Pb-isotopic growth curve at ~2140 Ma.

Four mineral separates from altered amphibolite, represented by calc-silicate rich phases and by hydrothermally altered and mineralised samples, have Pb-isotopic compositions that plot above the 1726 Ma isochron (diamonds in Fig. 5). This more radiogenic Pb-isotopic composition indicates admixture of a more evolved Pb component into the alteration fluids. The Pb-isotopic compositions of magnetite from an ultramafic rock and a magnetite skarn from the Qasigiannguit area plot below the isochron (out-

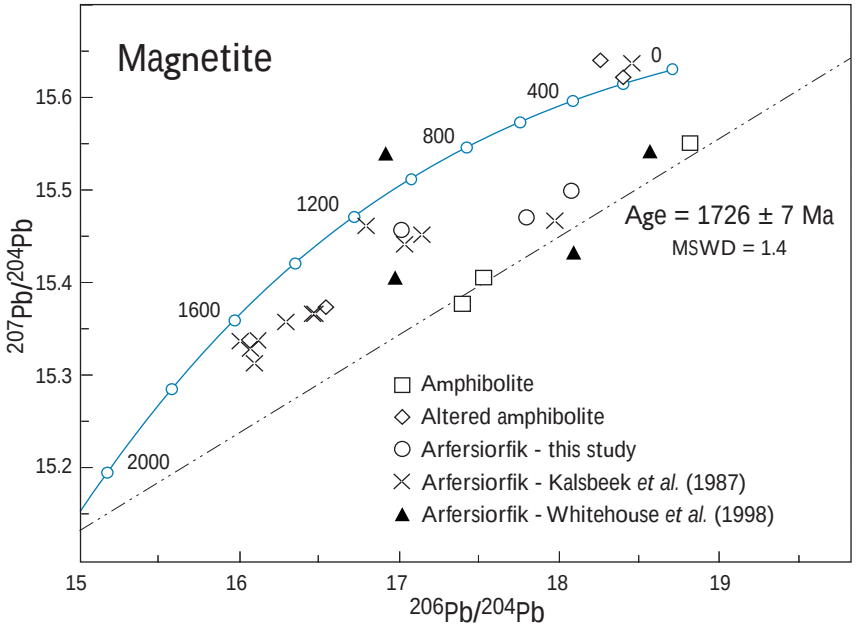

Fig. 5. $^{206}Pb/^{204}Pb$-$^{207}Pb/^{204}Pb$ diagram. Squares, Pb isotope ratios of magnetite from amphibolites; diamonds, magnetite from altered amphibolites (data from sample 446632 outside the range of Fig. 5, see Table 1). *Arfersiorfik quartz diorite:* circles, this study; crosses, data from Kalsbeek *et al*. 1987; filled triangles, data from Whitehouse *et al*. 1998. The isochron intercepts the Stacey & Kramers (1975) Pb-isotopic growth curve (blue) at ~2140 Ma.

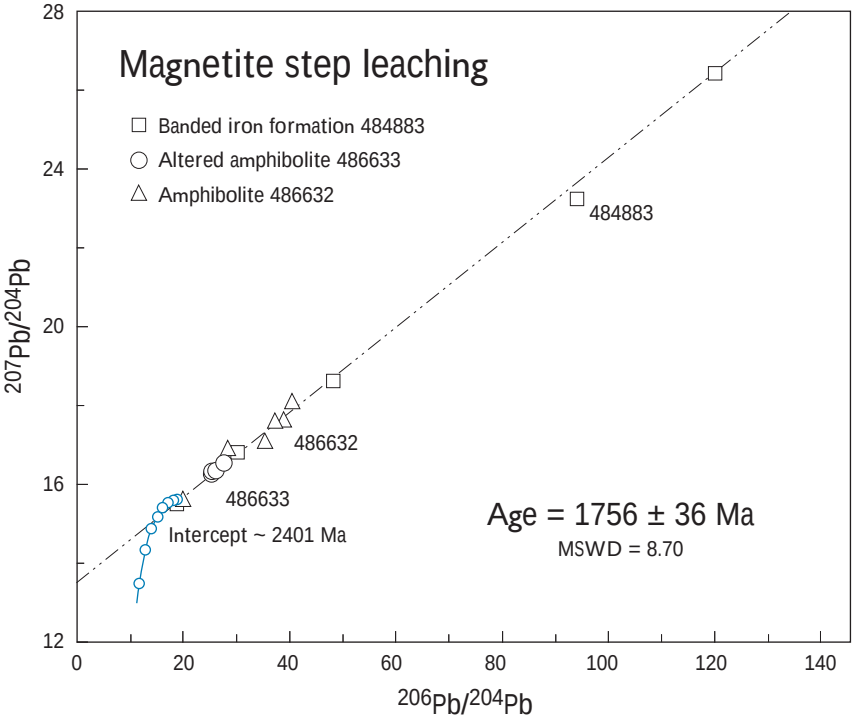

Fig. 6. $^{206}Pb/^{204}Pb$-$^{207}Pb/^{204}Pb$ diagram of step leaching results of magnetite for three samples. The errorchron intercepts the Stacey & Kramers (1975) Pb-isotopic growth curve (blue) at ~2400 Ma.

side the range of Fig. 5; see Table 1), suggesting a slightly more primitive Pb source.

The uranogenic vs. thorogenic isotopic patterns (not shown in a figure) are complex and do not add to a better understanding of the uranogenic Pb-isotopic data. As expected, they reflect differences in U/Th ratios among the different samples analysed.

The Arfersiorfik quartz diorite has been dated at ~1920 Ma (Kalsbeek *et al.* 1987). Three magnetite samples from this igneous suite have been included in the present study. The uranogenic Pb-isotopic compositions of these magnetites (circles in Fig. 5) are similar to the whole-rock Pb-isotopic signatures (crosses in Fig. 5; data from Kalsbeek *et al.* 1987). Four additional whole-rock analyses (filled triangles in Fig. 5; data of Whitehouse *et al.* 1998) show wider scatter than the data of Kalsbeek *et al.* (1987) and the results of this study.

The PbSL data obtained on magnetite from three of these samples are shown in Fig. 6. A regression for the steps defined by the sample of banded iron formation, 484883 (excluding step 3; Table 1) yields a best-fit line with a slope corresponding to an age of 1756 ± 36 Ma (MSWD = 8.70; model μ_1 = 7.70 ± 0.11; lower intercept with the Stacey & Kramers Pb-isotopic growth curve at ~2400 Ma), similar to the age obtained from the amphibolites. PbSL analyses of two other samples (446632, amphibolite and 446633, altered amphibolite) are closely scattered around the 1756 correlation line.

PbSL data obtained on allanite from a pink pegmatite (sample 2001-736) resulted in a well-defined errorchron with an age of 1818 ± 12 Ma (MSWD = 53.8; model μ_1 = 7.66 ± 0.02; lower intercept with the Stacey & Kramers Pb-isotopic growth curve at ~2450 Ma; Fig. 7A). The thorogenic vs. uranogenic isotopic pattern (Fig. 7B) reveals that essentially only one phase has dominantly contributed Pb to the leaching acids, as a nearly perfect linear relationship is indicated by the data points. This points to a more or less constant Th/U in the recovered Pb fractions. For this reason, the age of 1818 ± 12 Ma can be interpreted with great confidence to represent the emplacement age of the pegmatite. The Pb-isotopic composition of magnetite (sample 481087, Table 1) from this pegmatite plots on the allanite isochron (Fig. 7A), indicating preservation of isotopic equilibrium between these two phases.

PbSL data on monazite from a white pegmatite (sample 223736) also yield an errorchron, the slope of which corresponds to an age of 1797 ± 13 Ma (MSWD = 4.44; model μ_1 = 7.00 ± 0.05; lower intercept with the Stacey & Kramers Pb-isotopic growth curve at ~2925 Ma; Fig. 8A). The thorogenic vs. uranogenic isotopic pattern (Fig. 8B) again indicates a predominantly single phase that contributed Pb to the leaching acids, as the data points define a near perfect linear relationship. Consequently, with great confidence, the age of 1797 ± 13 Ma is interpreted as the intrusion age of this pegmatite.

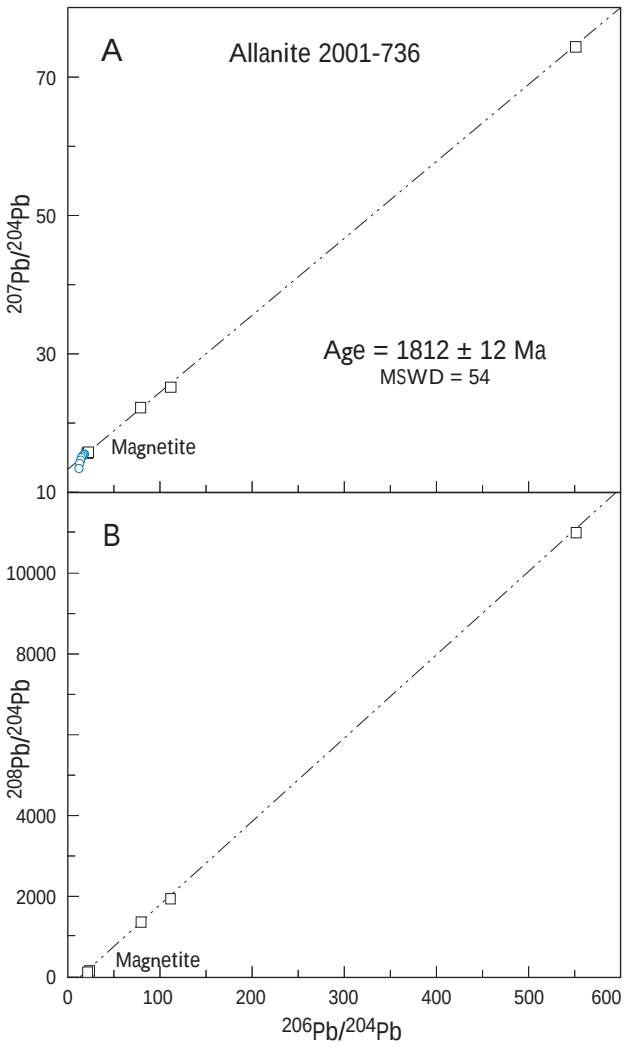

Fig. 7. Step leaching $^{206}Pb/^{204}Pb$-$^{207}Pb/^{204}Pb$ and $^{208}Pb/^{204}Pb$-$^{206}Pb/^{204}Pb$ diagrams of allanite from red pegmatite (sample 2000736). The errorchron intercepts the Stacey & Kramers (1975) Pb-isotopic growth curve (blue) at ~2925 Ma.

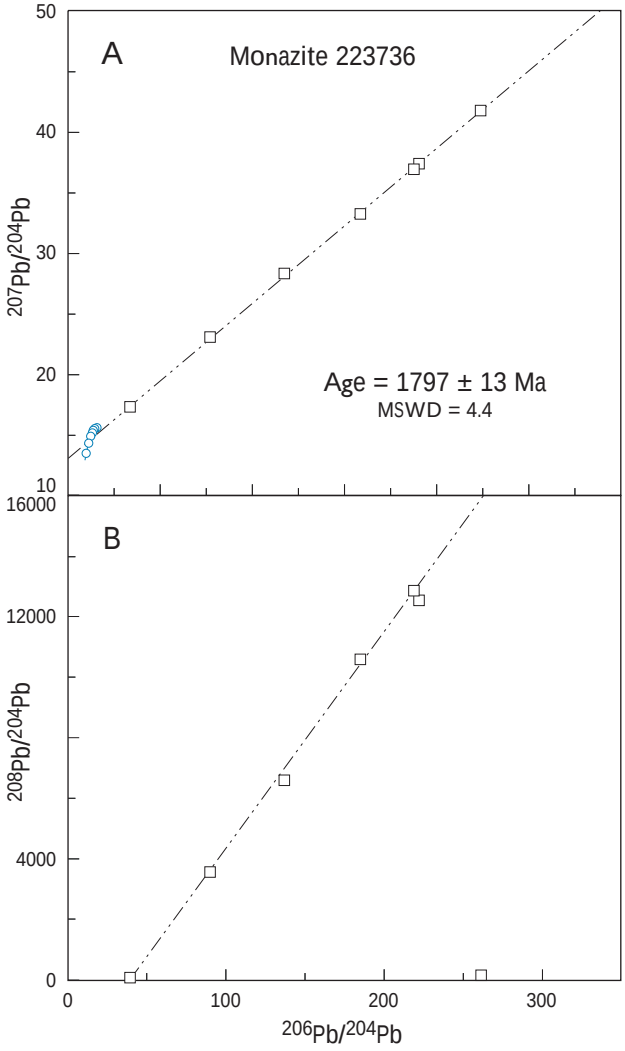

Fig. 8. Step leaching $^{206}Pb/^{204}Pb$-$^{207}Pb/^{204}Pb$ and $^{208}Pb/^{204}Pb$-$^{206}Pb/^{204}Pb$ diagrams of monazite from white pegmatite (sample 223736). The errorchron intercepts the Stacey & Kramers (1975) Pb-isotopic growth curve (blue) at ~2453 Ma.

Three more step-leaching experiments were performed on allanite (1) and monazite (2) separates from other pegmatites (Fig. 9). The ages defined by the respective errorchrons are similar to the ones presented above, and are close to 1800 Ma. Results of the isochron calculations are listed in Table 3.

Discussion

The age defined by the Pb-isotopic compositions of magnetite from the amphibolites (1726±7 Ma) is younger than the latest major tectonometamorphic event in the region (D4, strike-slip shearing and granite intrusion at 1780–1770 Ma; see Connelly *et al.* 2000 and van Gool *et al.* 2002), and may be interpreted as a cooling age after the D4 event. Metamorphic conditions in the CNO reached temperatures above 650°C at 1800 Ma and approximately 540°C by *c.* 1740 Ma (Connelly & Mengel 2000; Connelly *et al.* 2000; Willigers *et al.* 2001). Slow cooling followed with closing temperatures of rutile (420°C) around 1670 Ma (Connelly *et al.* 2000). Based on ^{40}Ar-^{39}Ar and U-Pb data of several minerals, Willigers *et al.* (2001) estimated cooling temperatures around 500°C at ~1700 Ma, 410°C at ~1640 Ma and 200°C at ~1400 Ma. A continuous magnetite-ulvöspinel solid solution series exists, with exsolution taking place below 600°C (Deer *et al.* 1966; Ramdohr 1969). Thus, the ages of the magnetite may date

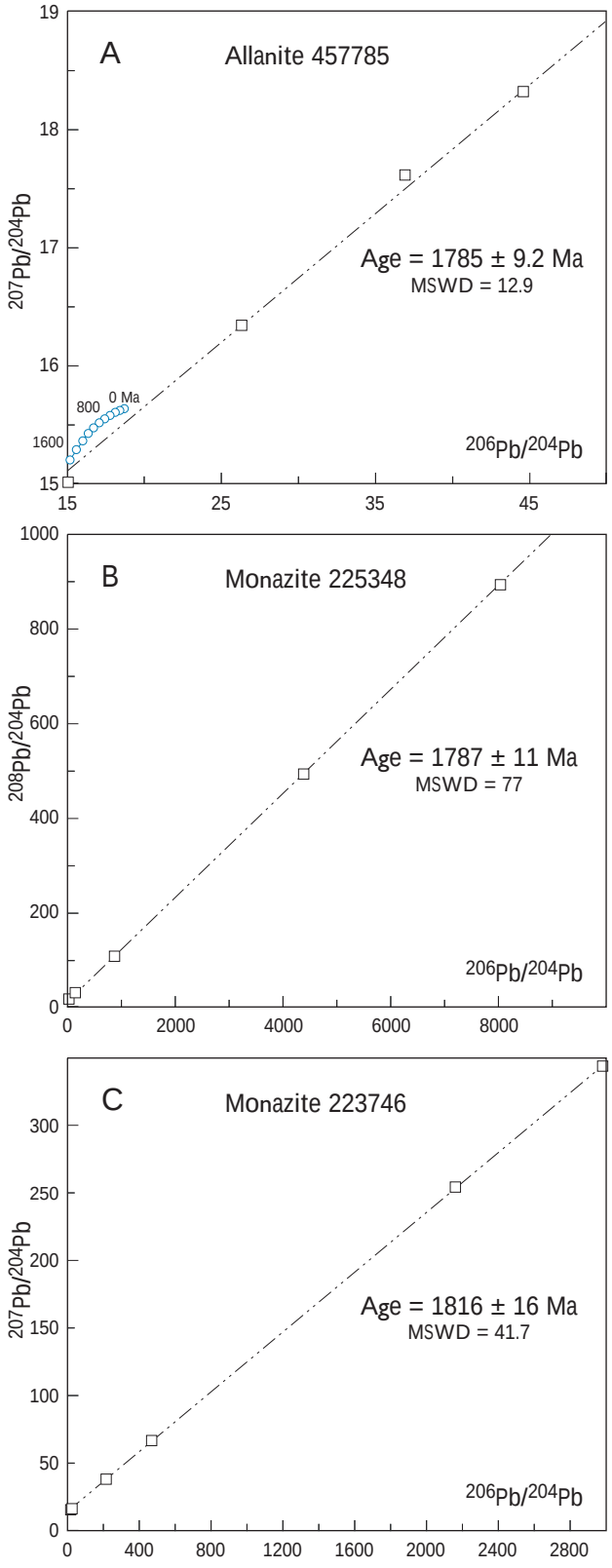

Fig. 9. Step leaching $^{206}Pb/^{204}Pb$-$^{207}Pb/^{204}Pb$ diagrams of monazite from white pegmatite (samples 225348 and 223736) and allanite from pink pegmatite (sample 447783). The errorchron intercepts of the Stacey & Kramers (1975) Pb-isotopic growth curve (blue) are given.

the timing where exsolution in magnetite ceased (< 1800 Ma), that is, after peak metamorphic conditions.

Model first-stage μ_1 values associated with Pb-Pb isochrons have been used elsewhere in Greenland to judge the influence of Pb from Archaean sources on the Pb-isotopic characteristics of Palaeoproterozoic igneous rocks (e.g. Kalsbeek & Taylor 1985). Rocks derived from Proterozoic sources commonly have model μ_1 values around 8, while contamination with Pb from Archaean sources tends to lower the μ_1 values. The high μ_1 value (7.89; Table 3) obtained for the amphibolite isochron and the lower intercept with Stacey & Kramers (1975) Pb-isotopic growth curve at 2140 Ma suggest a mainly Palaeoproterozoic Pb source for the amphibolites. This source is probably also related to the origin of the supracrustal rocks. Detrital zircon U-Pb ages of metasedimentary rocks of the Nordre Strømfjord suite (2200–1950 Ma; Nutman *et al*. 1999) and the Naternaq supracrustal belt (*c*. 1950–1900 Ma, Thrane & Connelly 2006, this volume) indicate erosion of a predominantly Palaeoproterozoic hinterland. It implies that the stratabound, semi-massive sulphide deposits associated with banded iron formation at Naternaq (Stendal *et al*. 2004) were also deposited during Palaeoproterozoic time.

The results of allanite and monazite PbSL experiments indicate pegmatite formation around 1800 Ma in both the CNO (at Nordre Strømfjord) and NNO (at Attu and Qasigiannguit). This is in agreement with ages reported by Kalsbeek & Nutman (1996) and Connelly *et al.* (2000), which are slightly younger (1780–1770 Ma) or within error overlapping those reported here. The pegmatites were emplaced after post-collisional deformation, large scale folding, and shear zone formation (D3) which ended around 1825 Ma (van Gool *et al.* 2002).

The wide range in model μ_1 values (7.00–7.81) and lower intercepts with the Stacey & Kramers (1975) Pb-isotopic growth curve (2271–2925 Ma) indicate variable contributions of Archaean and Palaeoproterozoic country rocks to the petrogenesis of the pegmatites: Pegmatite sample 223736 (μ_1 = 7.00; lower intercept at 2925 Ma) may largely consist of remelted Archaean country rock, whereas sample 225348 (μ_1 = 7.81; lower intercept at 2271 Ma) appears to be mainly derived from Palaeoproterozoic sources.

Hydrothermal activity in the region probably continued after the time of pegmatite emplacement and after the magnetite had cooled through its closing temperature (~600°C), which means that the temperatures of the hydrothermal fluids ranged from 650°C to 400°C in the period 1800–1650 Ma.

The Pb-isotopic signatures of the ultramafic rock and

the magnetite skarn from the Qasigiannguit area do not lend themselves to deduce whether these formations were formed during the Palaeoproterozoic or represent remnants of Archaean origin.

It has been suggested that many of the epigenetic gold and copper occurrences in the Ataa area north-east of Disko Bugt, about 75 km north of Jakobshavn Isfjord (Fig. 1), are contemporaneous with the peak metamorphism at ~1900 Ma in that area (Stendal 1998). This 1900 Ma metamorphic-hydrothermal event is not reflected in the magnetite Pb-isotopic data of the present study area.

Conclusions

Pb-isotopic data of magnetite can be related to the general geological evolution of the Nagssugtoqidian orogen and are thus a useful tool for studying the metamorphic history of Palaeoproterozoic events in West Greenland. A drawback of magnetite Pb-isotopic analysis, however, is the generally low Pb concentration in this mineral, which makes analysis difficult.

Magnetite in the amphibolites was formed during several stages of metamorphism. The isochron age of ~1726 Ma probably represents a cooling age after a prominent late tectonometamorphic event in the region dated at ~1775 Ma. The isotopic data suggest a Palaeoproterozoic (mantle?) source for the Pb in the amphibolites. The Nordre Strømfjord supracrustal suite, formed by erosion of a similar juvenile Palaeoproterozoic hinterland, was deposited between 2000 and 1920 Ma. It is suggested that the Naternaq sulphide deposit is part of this supracrustal suite.

Calc-alkaline magmatism related to subduction (1920–1870 Ma; Connelly *et al*. 2000) gave rise to the formation of the Arfersiorfik quartz diorite. The Pb-isotopic signature of magnetite from these rocks is comparable with that of whole-rock samples.

Allanite and monazite PbSL analyses yield pegmatite formation ages of ~1800 Ma for both the Nordre Strømfjord, Attu and Qasigiannguit regions. The formation of pegmatites is therefore post-collisional. The pegmatites were formed by melting of the local country rocks; Pb-isotopic data indicate that variable proportions of Late Archaean and Palaeoproterozoic age contributed to their petrogenesis. Hydrothermal activity continued after pegmatite emplacement and after closure of magnetite, at 1800–1650 Ma.

Acknowledgements

The authors acknowledge F. Kalsbeek for inspiring suggestions, and P.M. Holm and an anonymous reviewer for further improvements of the manuscript. This paper also contains contributions from several colleagues at GEUS, all of whom are acknowledged for their work. A special thanks goes to K. Markussen, Attu, for information about the allanite-bearing pegmatite south of the village.

References

Connelly, J.N. & Mengel, F.C. 2000: Evolution of Archean components in the Paleoproterozoic Nagssugtoqidian orogen, West Greenland. Geological Society of America Bulletin 112, 747–763.

Connelly, J.N., van Gool, J.A.M. & Mengel, F.C. 2000: Temporal evolution of a deeply eroded orogen: the Nagssugtoqidian orogen, West Greenland. Canadian Journal of Earth Sciences 37, 1121–1142.

Connelly, J.N., Thrane, K., Krawiec, A.W., & Garde, A.A. 2006: Linking the Palaeoproterozoic Nagssugtoqidian and Rinkian orogens through the Disko Bugt region of West Greenland. Journal of the Geological Society, London 163, 319–335.

Deer, W.A., Howie, R.A. & Zussman, J. 1966: An introduction to the rock-forming minerals, 528 pp. London: Longman.

Frei, R. & Kamber, B.S. 1995: Single mineral Pb-Pb dating. Earth and Planetary Science Letters 129, 261–268.

Garde, A.A. & Steenfelt, A. 1999: Precambrian geology of Nuussuaq and the area north-east of Disko Bugt, West Greenland. Geology of Greenland Survey Bulletin 181, 6–40.

Hollis, J.A., Keiding, M., Stensgaard, B.M., van Gool, J.A.M. & Garde, A.A. 2006: Evolution of Neoarchaean supracrustal belts at the northern margin of the North Atlantic Craton, West Greenland. In: Garde, A.A. & Kalsbeek, F. (eds): Precambrian crustal evolution and Cretaceous–Palaeogene faulting in West Greenland. Geological Survey of Denmark and Greenland Bulletin 11, 9–31 (this volume).

Kalsbeek, F. & Nutman, A.P. 1996: Anatomy of the early Proterozoic Nagssugtoqidian Orogen, West Greenland, explored by reconnaissance SHRIMP U-Pb zircon dating. Geology 24, 515–518.

Kalsbeek, F. & Taylor, P.N. 1985: Isotopic and chemical variations in granites across a Proterozoic continental margin – the Ketilidian mobile belt of South Greenland. Earth and Planetary Science Letters 73, 65–80.

Kalsbeek, F., Taylor, P.N. & Henriksen, N. 1984: Age of rocks, structures, and metamorphism in the Nagssugtoqidian mobile belt, West Greenland – field and Pb-isotope evidence. Canadian Journal of Earth Sciences 21, 1126–1131.

Kalsbeek, F., Pidgeon, R.T. & Taylor, P.N. 1987: Nagssugtoqidian mobile belt of West Greenland: cryptic 1850 Ma suture between two Archaean continents – chemical and isotopic evidence. Earth and Planetary Science Letters 85, 365–385.

Kalsbeek, F., Taylor, P.N. & Pidgeon, R.T. 1988: Unreworked Archaean basement and Proterozoic supracrustal rocks from northeastern Disko Bugt, West Greenland: implications for the nature of Proter-

ozoic mobile belts in Greenland. Canadian Journal of Earth Sciences 25, 773–782.

Ludwig, K.R. 1990: ISOPLOT for MS-DOS – A plotting and regression program for radiogenic isotope data, for IBM-PC compatible computers, version 2.03. United States Geological Survey, Open File Report OF-88-0557, 40 pp.

Nutman, A.P., Kalsbeek, F., Marker, M., van Gool, J.A.M. & Bridgwater, D. 1999: U-Pb zircon ages of Kangâmiut dykes and detrital zircons in metasediments in the Palaeoproterozoic Nagssugtoqidian orogen (West Greenland). Clues to the pre-collisional history of the orogen. Precambrian Research 93, 87–104.

Østergaard, C., Garde, A.A., Nygaard, J., Blomsterberg, J., Nielsen, B.M., Stendal, H. & Thomas, C.W. 2002: The Precambrian supracrustal rocks in the Naternaq (Lersletten) and Ikamiut areas, central West Greenland. Geology of Greenland Survey Bulletin 191, 24–32.

Ramdohr, P. 1969: The ore minerals and their intergrowths, 1174 pp. Oxford: Pergamon Press.

Schjødt, F. & Steenfelt, A. 2004: Mineral resources of the Precambrian shield of central West Greenland (66° to 70°15′ N). Part 1. Compilation of geoscience data. Danmarks og Grønlands Geologiske Undersøgelse Rapport 2004/16, 45 pp.

Secher, K. 1980: Distribution of radioactive mineralisation in central West Greenland. Rapport Grønlands Geologiske Undersøgelse 100, 61–65.

Stacey, J.S. & Kramers, J.D. 1975: Approximation of terrestrial lead isotope evolution by a two-stage model. Earth and Planetary Science Letters 26, 207–221.

Steenfelt, A., Stendal, H., Nielsen, B.M. & Rasmussen, T.M. 2004: Gold in central West Greenland – known and prospective occurrences. Geological Survey of Denmark and Greenland Bulletin 4, 65–68.

Stendal, H. 1998: Contrasting Pb isotopes of Archaean and Palaeoproterozoic sulphide mineralisation, Disko Bugt, central West Greenland. Mineralium Deposita 33, 255–265.

Stendal, H. & Schønwandt, H.K. 2003: Precambrian supracrustal rocks and mineral occurrences, north-east Disko Bugt. Danmarks og Grønlands Geologiske Undersøgelse Rapport 2003/24, 57 pp.

Stendal, H., Blomsterberg, J., Jensen, S.M., Lind, M., Madsen, H.B., Nielsen, B.M., Thorning, L. & Østergaard, C. 2002: The mineral resource potential of the Nordre Strømfjord – Qasigiannguit region, southern central West Greenland. Geology of Greenland Survey Bulletin 191, 39–47.

Stendal, H., Nielsen, B.M., Secher, K. & Steenfelt, A. 2004: Mineral resources of the Precambrian shield of central West Greenland (66° to 70°15′). Part 2. Mineral occurrences. Danmarks og Grønlands Geologiske Undersøgelse Rapport 2004/20, 212 pp.

Stendal, H., Frei, R. & Stensgaard, B.M. 2006: A lead isotope study of an Archaean gold prospect in the Attu region, Nagssugtoqidian orogen, West Greenland. In: Garde, A.A. & Kalsbeek, F. (eds): Precambrian crustal evolution and Cretaceous–Palaeogene faulting in West Greenland. Geological Survey of Denmark and Greenland Bulletin 11, 53–60 (this volume).

Taylor, P.N. & Kalsbeek, F. 1990: Dating the metamorphism of Precambrian marbles: Examples from Proterozoic mobile belts in Greenland. Chemical Geology 86, 21–28.

Thrane, K. & Connelly, J.N. 2006: Zircon geochronology from the Kangaatsiaq–Qasigiannguit region, the northern part of the 1.9–1.8 Ga Nagssugtoqidian orogen, West Greenland. In: Garde, A.A. & Kalsbeek, F. (eds): Precambrian crustal evolution and Cretaceous–Palaeogene faulting in West Greenland. Geological Survey of Denmark and Greenland Bulletin 11, 87–99 (this volume).

Todt, W., Cliff, R.A., Hanser, A. & Hofmann, A.W. 1993: Re-calibration of NBS lead standards using a 202Pb + 205Pb double spike. Terra Abstracts 5, Supplement 1.

van Gool, J.A.M., Connelly, J.N., Marker, M. & Mengel, F. 2002: The Nagssugtoqidian orogen of West Greenland: tectonic evolution and regional correlations from a West Greenland perspective. Canadian Journal of Earth Sciences 39, 665–686.

Whitehouse, M.J., Kalsbeek, F. & Nutman, A.P. 1998: Crustal growth and crustal recycling in the Nagssugtoqidian orogen of West Greenland: constraints from radiogenic isotope systematics and U-Pb zircon geochronology. Precambrian Research 91, 365–381.

Willigers, B.J.A., Krogstad, E.J. & Wijbrans, J.R. 2001: Comparison of thermochronometers in a slowly cooled granulite terrain: Nagssugtoqidian orogen, West Greenland. Journal of Petrology 42, 1729–1749.

Manuscript received 28 October 2004; revision accepted 19 December 2005